INTERNATIONAL JOURNAL OF
COASTAL & OFFSHORE ENGINEERING
IJCOE Vol.4/No. 2/Summer 2019 (55-63)

Available online at: www. Ijcoe.org

Capacity Evaluation of Ressalat Jacket of Persian Gulf Considering Proper Finite Element Modeling of Tubular Members

Mohammad Hadi Erfani [1] , Mohammad Reza Tabeshpour [2*], Hasan Sayyaadi [3]

[1] Ph.D. Student, Department of Mechanical Engineering, Sharif University of Technology; Erfani_mh@mech.sharif.edu*
[2] Associate Professor, Department of Mechanical Engineering, Sharif University of Technology; Tabeshpour@sharif.edu
[3] Professor, Department of Mechanical Engineering, Sharif University of Technology; Sayyaadi@sharif.edu

ARTICLE INFO

Article History:
Received: 11 May. 2019
Accepted: 10 Sep. 2019

Keywords:
Local Buckling
Pushover Analysis
Jacket Type Offshore Platforms
Compressive Behavior
ISO Equation

ABSTRACT

The capacity curve obtained from the pushover analysis of jacket-type offshore platforms gives their structural performance levels, ultimate capacity and ductility. Accurate estimation of structural capacity curve is of great importance. Accurate modeling of the global and local buckling of compression tubular members in a correct form is an effective part of studying the behavior of offshore jackets under all various types of loading conditions at any given time of their life. Modeling of compressive braces by shell or solid elements when the imperfections are applied leads to deformations due to local buckling based on buckling modes. This paper aims to achieve more accurate compressive behavior of compression members. The ABAQUS finite element software has been used for this purpose. Regarding to the results achieved from investigation of buckling in tubular members proper elements have been introduced to investigate the global and local buckling phenomena. Then pushovers results of Ressalat jacket with conventional modeling versus more accurate modeling proposed in this paper for compressive members have been compared as a case study. According to the results applying improper mesh size for compressive members can under-predict the ductility by 33% and under-estimate the lateral loading capacity up to 8%. Finally, ISO equations and Marshall strut theory have been applied to investigate critical buckling load and post-buckling response of tubular braces. The innovation of this paper is investigating the interaction of global and local buckling in the braces of jacket with 1-Dimentional elements using ISO equations and buckling envelope derived from the solid element results, which results in low computational costs.

1. Introduction

Critical buckling loads can be calculated for tubular members using empirical equations. These equations are presented by design codes such as API RP-2A WSD and API RP 2A-LRFD (recommended practice for planning, designing, and constructing fixed offshore platforms), ISO 19902 and NORSOK N-004 to achieve load and resistance design factors. All of these codes have been checked in order to assure that design loads do not meet critical buckling loads in normal and extreme operational conditions. Also both global elastic buckling and inelastic buckling are covered by design codes where prevent local buckling in walls of tubular members by decreasing the loads. Even to ensure that applied loads do not exceed the critical buckling loads in normal operations, these codes explain structural configuration of members.

Some members compress higher than their buckling limit under extreme load conditions such as ductility level earthquake (DLE[1]) and the results of this case on the behavior of the structure also need to be examined. It is possible that the structures are designed in such a way that local buckling occurs in some members under extreme loads. Subsequently, in the process of analysis, it is checked that the level of structural failure remains within acceptable limits. In this analysis, the actual response of the structure is obtained. For this purpose load factors and capacity factors are equal to 1. It is important that local buckling of members and their post-buckling behavior are detected, correctly. So that

[1] Ductility Level Earthquake

the load transfer to adjacent elements is not underestimated. Nonlinear finite element models with 1-D beam elements are usually used to analysis the collapse of jacket structures. But the beam elements do not consider the local buckling response and local deformation of walls of members. Local buckling often occurs in members with low ratio of diameter to thickness ratio (D/t). As the diameter to thickness ratio increases, local buckling is postponed to global buckling, and this event leads to a further drop in post-buckling capacity in comparison with the value that predicted by using the beam element. Also, models with beam elements cannot directly consider radial and circumferential imperfections due to fabrication tolerances which reduce load carrying capacity.

When shell elements are used to model thin-walled tubular members, the model elements is capable of considering global and local buckling at shell walls simultaneously.

The following is an overview of the researches that has been conducted to investigate the buckling of the tubular members. Karamanos and Tassoulas [1] derived curves concerning the capacity of tubular members using a nonlinear FE technique under the combination of external pressure and bending. Sadowski and Rotter [2] investigated the structural behavior of tubular columns under buckling phenomenon considering shell elements. Bardi and Kyriakides [3,4] studied the plastic buckling range of thick cylindrical shells. They focused on circular stainless steel tubes in both experimental and analytical phases. Yasseri and Skinner [5] in 2006 studied the global and local buckling of and their interaction for tubular members under concentrated force and moment. They classified the compressive members based on the diameter to thickness ratio (D/t) and the ratio of length to gyration radius (L/r). They proposed the suggested API curve of elastic and non-elastic buckling based on the slenderness. They also studied the effects of the imperfection of compressive members. The modified properties of steel material which can be used for beam elements to achieve the same response of shell elements have been also presented in that report. Wenjing and Hoogenboom [6] in 2011 checked the buckling of the frame members when the buckling length has been set manually. Based on their estimation, 5 to 10% of the man-hours in structural analysis of removal projects has been spent on checking and correcting buckling lengths. Using another method is available that does not require determining buckling lengths. In the study, the NORSOK standard for tubular steel frame structures has been used to derive this method. They concluded that this method can be successfully applied. In this paper, for a 2-D frame of a typical jacket platform, the global and local buckling of models developed by using shell or beam elements are compared. Also, the responses of beam elements that can consider the effects of local buckling are obtained. For this purpose, the Marshall strut theory in the ABAQUS finite element software suite is used.

2. Analytical models

Two types of second-order shell and beam elements have been used to develop the models. Frame elements have been used to reflect the effect of local buckling that it can be formed well in the walls of tubular parts ,modeled by shell elements, because of local deformations. The most important difference of beam elements compared to frame elements, is that frame elements use ISO 19902 buckling equations in addition to the beam elements equations. Also, in terms of numerical modeling, the number of frame elements is limited to one mesh element in length. After the buckling happens, the response of standard frame element is switched to the buckling strut response and is never switched back again. If the buckling strut response is requested for the element from the first step of the analysis, the member will be changed to a simply-supported member, so that the member cannot resists against bending moments. The proper meshing of elements in a model provides optimum precision. When a fine-meshed shell model is used, local buckling occurs earlier than beam models and also does not reach the same post-buckling strength in the load-displacement graph. But frame elements correct this deficiency of beam elements and also reduce the computational costs.

A primary imperfection equal to 0.1% of member length has been applied to the compressive members of shell and beam elements to consider the buckling phenomena. It is necessary first to obtain probable buckling modes by calculating the eigenvalues of the model, in order to determine the locations of imperfe-ctions. The models with frame elements do not require applying the imperfection; these types of elements consider both elastic and inelastic buckling.

The mesh size is almost the same at both models of shell elements and beam-frame elements, So that the results are better comparable. Of course, it should be noted that frame elements only have a single mesh along its length.

3. Analysis method

The static Riks analysis method has been used in ABAQUS software because the other analysis methods become unstable under a sudden reduction in stiffness due to buckling. In the Riks procedure, deformations and loads are considered simultaneous-ly. This means that the magnitude of the load is taken as a variable and the arc length method, in a static equilibrium in the load-displacement space, is used to obtain the solution [7]. So, the ABAQUS program is able to discover the post-buckling response of the model by reducing the applied load and solving the load-displacement equation.

The models of beam and shell elements with and without imperfection are analyzed by this method. And the buckling and post-buckling responses of both element types are compared.

4. Loading

The purpose of this paper is to estimate the pushover curve of the structure by enforcing lateral displacement and extracting the base shear. This lateral displacement can be imposed on solitary node placed on highest deck of jacket or distributed to all nodes at different levels of the platform along the height. In each case the reaction forces at the level of the fixed supports at the bottom of piles, which is the base shear and equal to the total load applied to the platform, have been calculated. Therefore, the approach of displacement-control has been adopted in this paper. So, ductile behavior of structure can be observed correctly in load-displacement curve obtained from pushover analysis. Fig. 1 illustrates two distributions of lateral displacement applied in this paper.

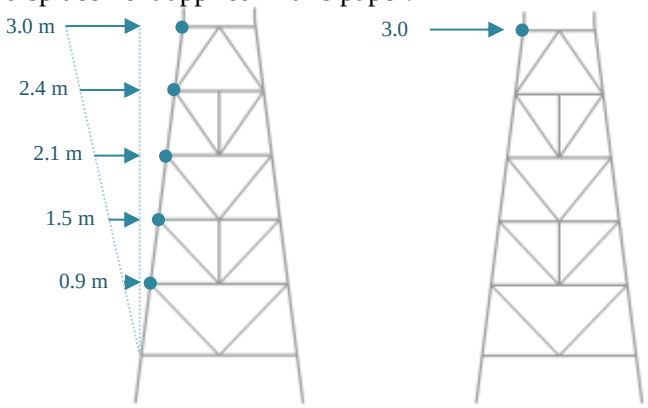

Figure 1. Two types of distribution of lateral displacement applied in FE models

5. Material properties

Almost all the elements have been defined by yield stress of 355 MPa and ultimate strength of 535 MPa at a plastic strain of 0.144. The narrowing test of the coupon bar under axial load is used to obtain true stresses. The values of true stresses and logarithmic strains are calculated from the nominal experimental values using the following equations.

$$\sigma_{true} = \sigma_{nom}(1 + \varepsilon_{nom}) \quad (1)$$

$$\varepsilon_{ln}{}^{pl} = \ln(1 + \varepsilon_{nom}) - \sigma_{nom}/E \quad (2)$$

6. Buckling prediction, analytical equations

This part describes the ISO equation in detail, but the differences of the approach of other standards have been explained [8]. All four codes (API RP-2A WSD, API RP 2A-LRFD, ISO 19902 and NORSOK N-004) provide sets of formulations for each load type acting alone or in combination. The ISO equation is used with a high accuracy to predict the onset of buckling in slender members with pipe-like cross-sections. All quantities with dimensions have dimensions of stress.

$$\frac{\gamma_{R.c}\sigma_c}{f_c} + \frac{\gamma_{R.b}}{f_b}\left[\left(\frac{C_{m.y}\sigma_{b.y}}{1-\sigma_c/f_{e.y}}\right)^2 + \left(\frac{C_{m.z}\sigma_{b.z}}{1-\sigma_c/f_{e.z}}\right)^2\right]^{0.5} \leq 1.0$$

and (3)

$$\frac{\gamma_{R.c}\sigma_c}{f_{yc}} + \frac{\gamma_{R.b}\sqrt{\sigma_{b.y}^2 + \sigma_{b.z}^2}}{f_b} \leq 1.0$$

Here, f_c is the characteristic axial compressive stress, f_b is the characteristic bending stress, c_{m1} and c_{m2} are reduction factors corresponding to the cross-section directions 1 and 2, and F_{e1} and F_{e2} are the Euler buckling stresses corresponding to the 1 and 2 directions.

$$I_{11} = I_{22} = \frac{\pi}{64}(D^4 - (D - 2\,t)^4) \quad (4)$$

$$Z_e = \frac{\pi}{64}(D^4 - (D - 2\,t)^4)/\left(\frac{D}{2}\right) \quad (5)$$

$$Z_p = (D^3 - (D - 2\,t)^3)/6 \quad (6)$$

$$r = \sqrt{I_{22}/A} = \frac{1}{4}\sqrt{(D^2 - (D - 2\,t)^2)} \quad (7)$$

Local buckling check in ISO and NORSOK is based on material as well as geometric properties of members whereas in API WSD and API LRFD it depends on only geometry parameters. Therefore, the terms of the ISO equation are calculated as follows:

$$f_c = P/A \quad (8)$$

$$f_{bi} = M_i/Z_e \quad (9)$$

$$F_{yc} = f_y \quad \text{for} \quad \frac{f_y}{F_e} \leq 0.17$$

$$F_{yc} = \left(c_2 - c_3\frac{f_y}{F_e}\right)f_y \quad \text{for} \quad \frac{f_y}{F_e} \leq 1.911 \quad (10)$$

$$F_{yc} = F_e \quad \text{for} \quad \frac{f_y}{F_e} > 1.911$$

$$c_2 = 1.04654873 \quad \& \quad c_3 = 0.27381606 \quad (11)$$

$$F_e = 2CE\left(\frac{t}{D}\right) \quad \& \quad C = 0.3 \quad (12)$$

Where, F_{yc} is the local buckling strength and for $\frac{f_y}{F_e} > 1.911$ the F_{yc} is equal to the elastic local buckling strength (F_e). There is only a slight difference in limitation between ISO and the NORSOK code but both of them have the same approach. API WSD and LRFD codes distinguish between elastic and inelastic buckling stresses. The inelastic local buckling stress formula proposed by API WSD and LRFD codes is as follows:

$$F_{yc} = f_y \quad \text{for} \quad \frac{D}{t} \leq 60$$

$$F_{yc} = \left(1.64 - 0.23\left(D/t\right)^{1/4}\right)f_y \leq F_e \quad (13)$$

$$\text{for} \quad 60 < \frac{D}{t} < 300;\ t \geq 6\,mm$$

In the above local buckling equations, ISO and NORSOK codes limit D/t to a maximum of only 120, whereas the API increase the upper limit of D/t ratio to 300 meaning that NORSOK is significantly more conservative.

$$F_c = [1 - 0.278\lambda^2]F_{yc} \quad \text{for} \quad \lambda \leq 1.34 \quad (14)$$

$$F_c = \frac{c_1}{\lambda^2}F_{yc} \quad \text{for} \quad \lambda > 1.34$$

$$\lambda = \max(\lambda_1, \lambda_2) \quad \& \quad c_1 = 0.89282978 \quad (15)$$

$$\lambda_i = \frac{k_i L_i}{\pi r}\sqrt{\frac{F_{yc}}{E}} \quad (16)$$

Where, F_c is the representative axial compressive strength, in stress units; λ is the column slenderness parameter. The two API LRFD and NORSOK codes recommend formulae similar to ISO form but employ different coefficients. The overall column buckling formula in API WSD uses the AISC formulation, while API LRFD, ISO and NORSOK are limit state design (LSD) or LRFD based. The NORSOK recommended equation gives lower capacity than API LRFD and ISO. Unlike the other three standards, NORSOK code assumes that the platform is manned even during extreme environmental events, so in calculation of both local and overall buckling strength, NORSOK is more conservative. The API WSD formula in accordance with AISC is as follows:

$$F_c = \frac{\left[\left(1-\left(Kl/r\right)^2\right)/\left(2C_c^2\right)\right]}{5/3+3\left(Kl/r\right)/(8C_c)-\left(Kl/r\right)^3/(8C_c^3)} f_y \qquad \text{for } \frac{Kl}{r} < C_c \quad (17)$$

$$F_c = 12\pi^2 E/\left[23\left(Kl/r\right)^2\right] \qquad \text{for } Kl/r > C_c$$

$$C_c = \left(2\pi^2 E/f_y\right)^{1/2} \quad (18)$$

$$F_b = \left(Z_p/Z_e\right)f_y \quad \text{for } \frac{f_y D}{Et} \le 0.0517$$

$$F_b = \left(c_4 - 2.58\left(\frac{f_y D}{Et}\right)\right)\left(Z_p/Z_e\right)f_y \quad \text{for } 0.0517 < \frac{f_y D}{Et} \le 0.1034 \quad (19)$$

$$F_b = \left(c_5 - 0.76\left(\frac{f_y D}{Et}\right)\right)\left(Z_p/Z_e\right)f_y \quad \text{for } 0.1034 < \frac{f_y D}{Et} \le 120\frac{f_y}{E}$$

$$c_4 = 1.133386 \quad \& \quad c_5 = 0.945198 \quad (20)$$

Where, F_b is the bending strength. The formulae from all four codes are the same but the API WSD has different coefficients. According to above equations, elastic section modulus, plastic section modulus and yield strength can be seen in formulae because LSD and LRFD approaches consider full plasticity and yielding in the section, whereas because of WSD methodology which limits the stress to a fraction of the yield, only the yield strength exist in API WSD equations.

Also in evaluation of bending capacity NORSOK is more conservative than three others.

$$F_{ei} = \frac{F_{yc}}{\lambda_i^2} \quad (21)$$

Where, C_{m1} and C_{m2} are reduction factors corresponding to the cross-section directions 1 and 2. These factors are functions of the end moments, compressive stress and Euler buckling stresses with the default values of 0.85. By satisfying the following condition:

$$I(f_c, f_{b1}, f_{b2}) = 1.0 \quad (22)$$

Standard frame element response is switched to the buckling strut response and is never switched back again. The ISO equation yields the critical load, P_{cr}, which is defined as $f_c A$. When the axial forces are negligible and the bending moments have large values, another inequality is also used. This additional control is called the strength equation and is as follows:

$$S = \frac{f_c}{F_{yc}} + \frac{1}{F_b}\sqrt{f_{b1}^2 + f_{b2}^2} \quad (23)$$

The API WSD, ISO and NORSOK codes formulae have the same linear form with some partial differences, while API LRFD recommends a cosine form equation.

Both the following equations must be satisfied (I=1.0 and S≤1.0) to switch to the buckling strut behavior for a frame element.

$$I = 1.0 \quad (24)$$

$$S \le 1.0 \quad (25)$$

If the buckling strut response is requested for the element from the first step of the analysis, the member will be changed to a simply-supported member and the bending moments cannot be supported by the member. In this state, the ISO equation turns into the following simple equation.

$$P_{cr} = F_c A \quad and \quad f_c < F_c \quad (26)$$

6.1. Marshall Strut Envelope

The Marshall strut envelope defines the post-buckling damaged elasticity model and the hysteretic loop response [9]. To define the Marshall strut envelope, the value of P_{cr} and the following seven constants are needed:

ξ: is the coefficient defining $P_y = \xi\sigma^0 A$ ($\xi = 0.95$)

γ: is the isotropic hardening slope coefficient (0.02),

α_0: is the coefficient defining= $\alpha_0 + \alpha_1 \frac{L}{D}$

α_1: is the coefficient defining= $\alpha_0 + \alpha_1 \frac{L}{D}$, ($\alpha_0 = 0.03$) , ($\alpha_1 = 0.004$)

κ: is the force coefficient (0.28),

β: is the slope coefficient (0.02), and

ζ: is the force coefficient ($\min\left(1.0\,, 5.8\left(\frac{t}{D}\right)^{0.7}/\xi\right)$).

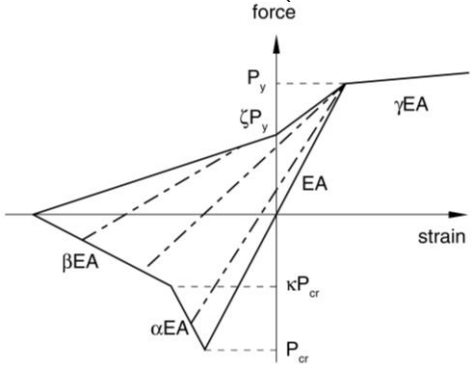

Figure 2. Marshall strut theory buckling envelope

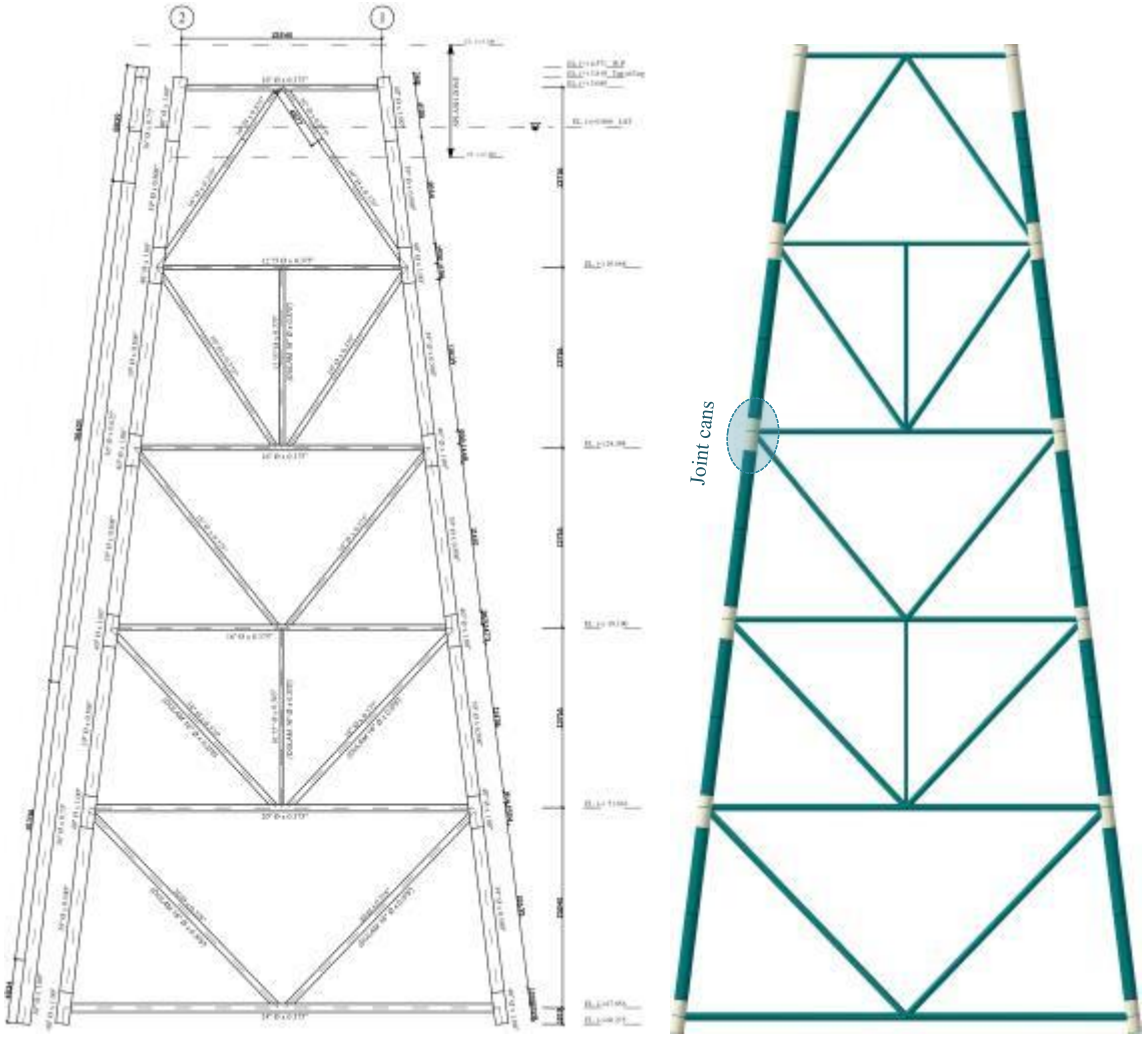

Figure 3. Schematic geometry of one row of Ressalat jacket and FE model

The values in parentheses are the default values supplied by ABAQUS, and the value of P_{cr} is found from the ISO equation as explained above. The Marshall envelope governs the compressive and tensile response of the strut as shown in Fig. 2. The dotted lines in the interior of the envelope indicate the damaged-elastic modulus defining the loading-unloading force versus strain path [10].

7. Modeling

A 3-Dimensional model of one frame of a four-leg Ressalat jacket platform of Persian Gulf has been performed. The schematic geometry and dimensions of the platform are shown in Fig. 3. All of the joint cans and the principal details have been taken into account in FE modeling.

Regarding to aspect ratios of sections used in the model, the maximum and minimum L/r ratio of the compressive braces are 126.01 and 118.63, respectively.

In this paper, the FE modeling of jacket is categorized into three main steps. On the first step, the jacket has been modeled using common two-node linear beam elements and 3D shell element both of which have been meshed with the common and traditional mesh size. The mesh size selected in this step is extensively applied in FE modeling of wide range of papers. Afterwards, in the second step the shell elements with optimized mesh size based on the previous studies of the authors [11,12,13,14], were replaced with the compressive braces of the platform. The mesh sizes applied in the second step can properly predict the buckling occurrence and post-buckling strength of braces. Changes in the structural behavior of the jacket have been considered at this step and represent below. Finally, in the third step all the braces have been replaced by two-node frame elements. The buckling behavior of each frame element has been achieved according to buckling behavior of respective brace model with 3D shell elements and Marshal strut envelope. Applying two-node frame elements conducts the models toward reducing the run time and costs of analysis. Pushover analysis has been executed as an approach to distinguish variations of results in different steps. The main deck has been simulated on the upper end of the piles in the form of a rigid connection between pile heads. Two concentrated masses have been applied on pile heads. Each of them has been assumed equal to 25% of the total mass of the platform deck, i.e. 2500 tones.

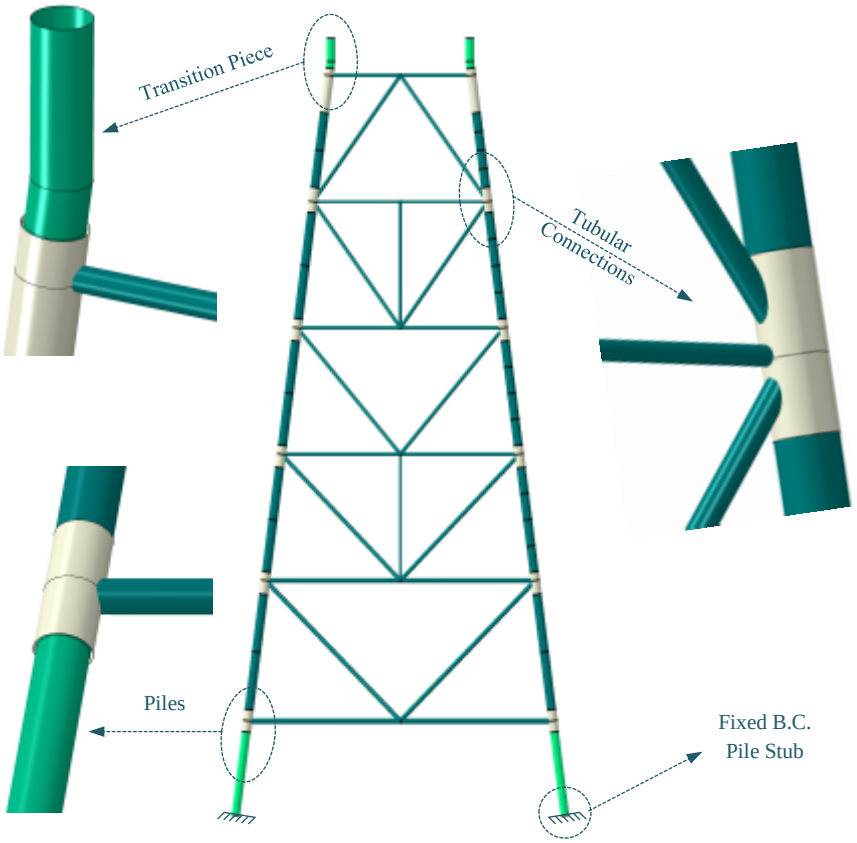

Figure 4. Model view of shell elements include global geometry of model, geometry of piles driven into legs, geometry of transition piece, and the geometry of one tubular connection

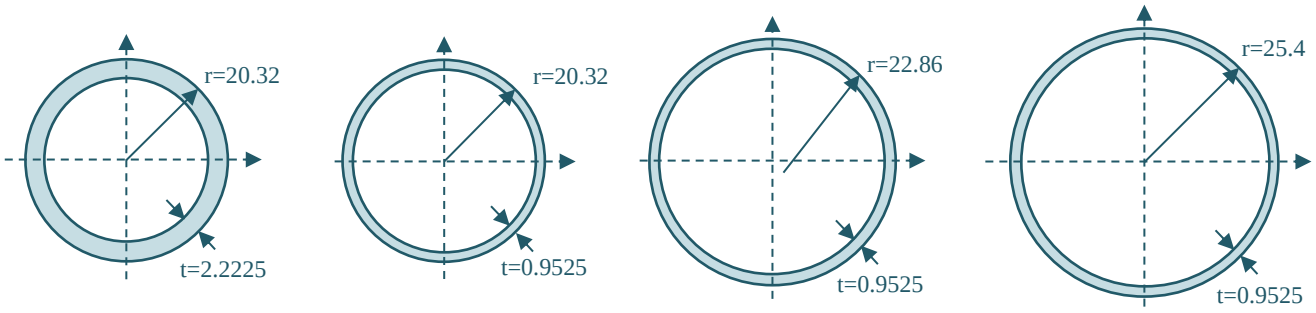

Figure 5. Geometry of all types of the frame elements cross-sections. All quantities have dimensions of cm.

Jackets and piles have been modeled separately and the cylindrical connection has been defined between them so that the piles can drive freely into the legs in rotational and translational degrees of freedom. In all the models, the pile stub technique has been used and the fixed end point of the piles has been set at a depth equal to 10 times its diameter. Fig. 4 shows the geometry modeled with shell elements.

The schematic view of all types of cross-section geometries defined for frame elements have been shown in Fig. 5.

8. Results

The critical buckling loads obtained from the numerical models with frame elements have been compared with the results of the ISO equation. Eventually, the most differences in all cases have been limited to 2 percent.

Failure due to elastic buckling of the member occurs prior to material yielding by increasing the length to radius of gyration ratio (L/r) in long members ($L/r > 100$). In long members the critical buckling force can be predicted by the Euler formula [15]:

$$P_{cr} = \frac{n\pi^2 EI}{Le^2} \quad (27)$$

For tubular members with intermediate length ($40 \leq L/r \leq 100$), the material reaches its limit of proportionality at the outer fiber of the member leading to a reduction in stiffness and kneeling of the section. So, the Euler formula overestimates critical buckling force. Fig. 6 displays a comparison between the typical elastic and inelastic buckling shapes. Also this figure demonstrates the variation of critical buckling load versus column slenderness parameter, λ.

In short braces ($L/r < 40$), the section may meets the yielding before occurrence of buckling.

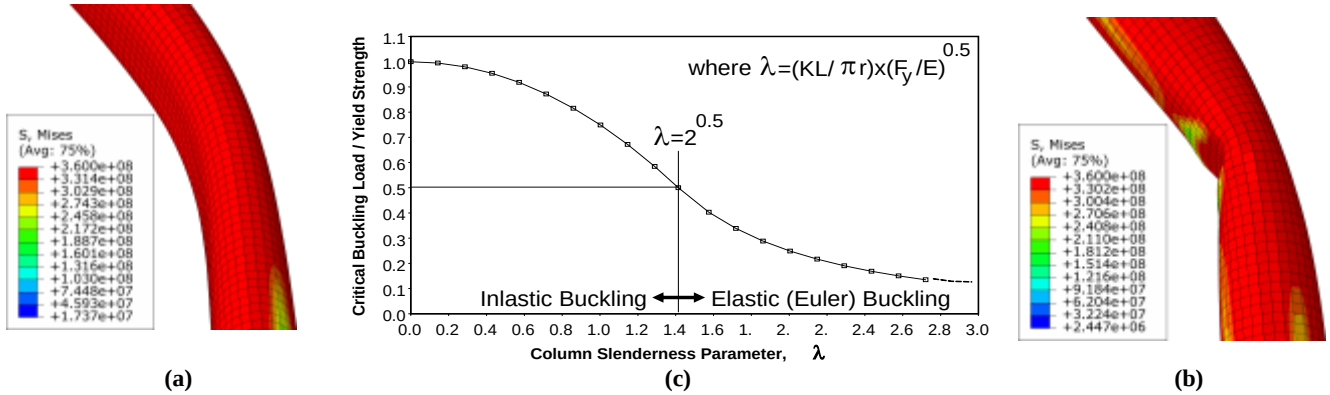

Figure 6. A sample of comparison between elastic and inelastic buckling shape; (a) Elastic buckling (long braces) (b) Inelastic buckling/kneeling (intermediate/short braces) (c) The critical buckling load versus column slenderness parameter

In these members the buckling shape will be similar to the elements with moderate length. However, in short members a larger area around the buckled section meets the yield level.

By increasing the D/t ratio the flexural stiffness of shell wall decreases with a power of 3 [5]. After occurrence of the buckling, the shell walls start to swing and ultimately the member bends. Local flexural moments due to deformation of the shell wall quickly result a local plastic zone. Finally, the local buckling which reduces the capacity of member leads to global buckling.

Increasing the L/r ratio results in further plastic zone and fewer critical buckling load. The enlarged plastic area causes a sudden collapse if the local buckling occurs in this state [5].

Fig. 7 and Fig. 8 present the results of the pushover analysis performed on the three separate steps explained before. In Fig. 7 the distribution of lateral displacement which defined in FE model is triangular and has ascending order in height with a maximum displacement of 3 m in the main deck. While Fig. 8 illustrates the results of pushover analyzes with a point-centered lateral displacement of 3 m at the level of main deck. Both of distributions are in accordance with pictures shown in Fig. 1.

The order of buckling occurrence in braces is displayed in the Fig. 7. The buckling of the compressive brace positioned at the lowest level of the jacket causes immediate drop and severe loses of global capacity throughout the structure. The buckling of this brace has not been observed when proper mesh has been assigned to all braces. Therefore, a sharp drop in pushover capacity curve has not occurred in models with proper mesh and models contain frame elements. According to the Fig. 7 applying improper mesh size for compressive members can under-predict the ductility by 33% and under-estimate the lateral loading capacity up to 8%. Each of the braces in model with typical and inappropriate mesh, buckled earlier than model with proper mesh.

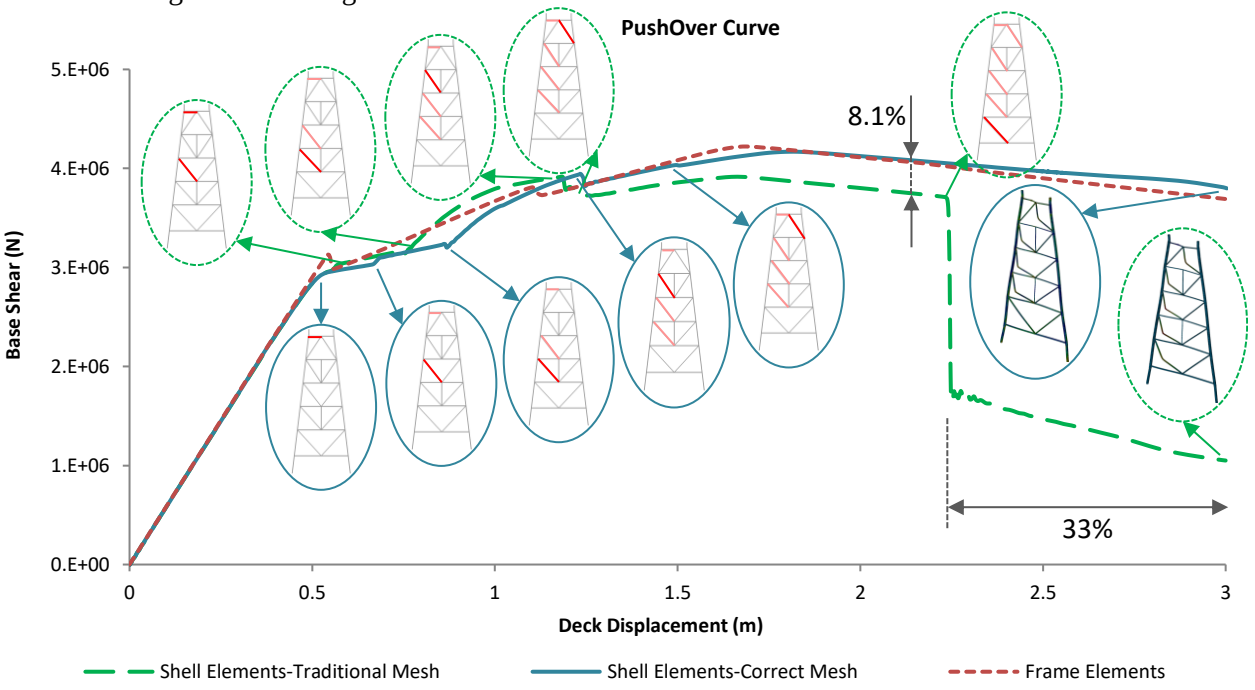

Figure 7. Results of pushover analysis of models with frame and shell elements for push distribution type 1

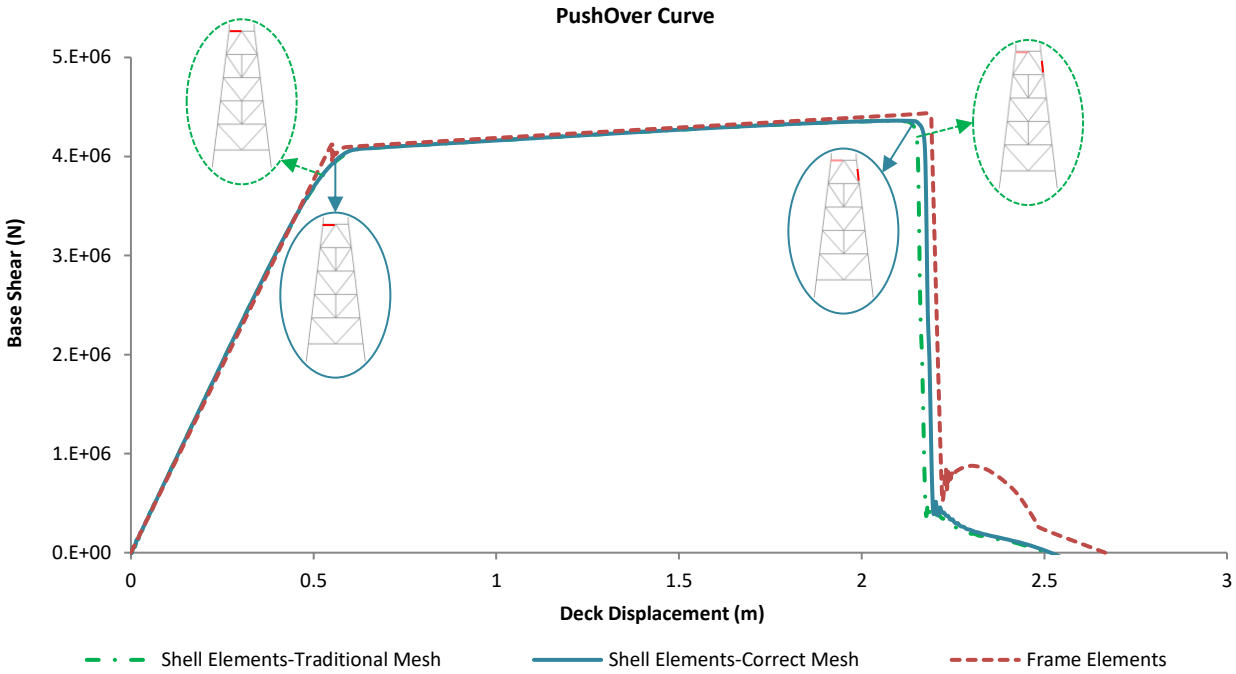

Figure 8. Results of pushover analysis of models with frame and shell elements for push distribution type 2

As seen in Fig. 8 the point-centered lateral push of jacket, did not actuate the compressive capacity of braces and no buckling can be seen in the braces of jacket. Finally, only damage occurrence in the pile at top level causes immediate resistance loss and global collapse of the structural. Also at this distribution the frame elements can properly consider the buckling capacity of braces due to investigation of the effects of local buckling along with global buckling. Besides that utilization of frame element can significantly decreases the time and cost of analysis and modeling.

9. Conclusions

It is proved that the frame elements consider interaction of local and global buckling using ISO equation and Marshall's buckling theory that is described in detail in the paper. However based on the results obtained from the models, it is possible that frame elements do not provide accurate prediction of buckling and post-buckling behavior of structures by incorrect estimation of various parameters of Marshal's curve. It should be noted that the use of frame elements greatly reduces the analysis costs than those using shell elements. On the other side, applying proper mesh in structural FE modeling of jackets with 3D shell or solid elements will affect the accuracy of the estimation of capacity curve including two important items of ultimate lateral bearing and ductility and finally the structural performance levels derived from this curve. Number of mesh elements on section and the ratio of element size along the member length to section are two fundamental parameters in modeling of compressive members with 3D shell elements. Improper determination of these values for braces of jacket could under-predict the ductility by 33% and under-estimate the lateral loading capacity up to 8%. But due to damage occurrence in piles, the behaviors of jackets with different mesh size are almost the same when the lateral push of the structure concentrated on the level of main deck.

List of Symbols

D	outer diameter
t	wall thickness of pipe
P	axial force
σ^0	yield stress
E	Young's modulus of elasticity
A	cross-sectional area
Z_e	elastic section modulus
k_1, k_2	effective length factors in the 1 and 2 directions
Z_p	plastic section modulus
L_1, L_2	unbraced lengths for the 1 and 2 directions
r	radius of gyration
I_{11}, I_{22}	bending moment of inertia in 1 and 2 directions

10. References

1- Karamanos, S.A., Tassoulas, J.L., (1996), *Tubular members II: local buckling and experimental verification*, Journal of engineering mechanics, 122(1), p. 72-78.

2- Sadowski, A.J., Rotter, J.M., (2013), *solid or shell finite elements to model thick cylindrical tubes and shells under global bending*, International journal of mechanical sciences, 74, pp.143-153.

3- Bardi, F.C., Kyriakides, S., (2006), *Plastic buckling of circular tubes under axial compression—part I:*

experiments, International journal of mechanical sciences, 48(8), pp.830-841.

4- Bardi, F.C., Kyriakides, S., Yun, H.D., (2006), *Plastic buckling of circular tubes under axial compression—part II: analysis*, International journal of mechanical sciences, 48(8), pp.842-854.

5- Yasseri, S., Skinner, K., Styles, D., (2006), *Post buckling response study for high D/t tubular members*, Technical report.

6- Xia, W. and Hoogenboom, P.C.J., (2011), *Buckling analysis of offshore jackets in removal operations*, ASME 2011 30th International Conference on Ocean, Offshore and Arctic Engineering (pp. 449-454), American Society of Mechanical Engineers.

7- Fernando, P., Rodrigues, N., Jacob, BP., (2005), *Collapse analysis of steel jacket structures for offshore oil exploitation*, Journal of constructional steel research, 61.

8- (2007), *ISO 19902*, International Standard: Petroleum and natural gas industries-fixed steel offshore structures, First edition.

9- Marshall, P.W., (1992), *Design of welded tubular connections, basis and use of AWS code provisions*, Elsevier.

10- Simulia, D.S. (Dassault Systèmes), (2012), *Abaqus 6.12 documentation*, Providence, Rhode Island, US, 261.

11- Tabeshpour, M.R., Erfani, M.H., Sayyadi, H., (2016), *Study on ultimate capacity of offshore jacket platforms by using beam elements, considering the effects of global and local buckling of the elements*, 18th international conference of marine industries (MIC2016), Kish Island.

12- Tabeshpour, M.R., Erfani, M.H. and Sayyaadi, H., (2019), *Challenges in calculation of critical buckling load of tubular members of jacket platforms in finite element modeling*, Journal of marine science and technology, pp.1-21.

13- Tabeshpour, M.R., Erfani, M.H. and Sayyadi, H., (2019), *Study on ultimate capacity of offshore jacket platforms considering the effects of general and local buckling of the elements*, Advances in Solid and Fluid Mechanics., 1(1), pp.9-17.

14- Tabeshpour, M.R., Erfani, M.H. and Sayyadi, H., (2018), *Investigation of uncertainties in buckling and post-buckling behavior of typical braces of offshore jacket platforms by using solid elements in ABAQUS*, 20th international conference of marine industries (MIC2018), Tehran.

15- Su, R.K. and Wang, L., (2015), *Flexural and axial strengthening of preloaded concrete columns under large eccentric loads by flat and precambered steel plates*, Structure and infrastructure engineering, 11(8), pp.1083-1101.